35th EPS Conference on Plasma Phys. Hersonissos, 9 - 13 June 2008 ECA Vol.**32D**, P-2.105 (2008)

# Implementation of sheath effects into TOPICA

B. Van Compernolle[1], R. Maggiora[2], G. Vecchi[2], D. Milanesio[2] and R. Koch[1]

[1]*Laboratory for Plasma Physics - Association 'Euratom-Belgian State'*
*Ecole Royale Militaire - Koninklijke Militaire School, B-1000 Brussels, Belgium*[*]

[2]*Politecnico di Torino, Dipartimento di Elettronica, Torino, Italy*

[*] *Partner in the Trilateral Euregio Cluster (TEC).*

## Introduction

Recent experiments [1] have shown that anomalous power losses and hot spots can occur due to the acceleration of ions into the antenna walls by RF sheath potentials. Parametric studies [1] show that temperature increases on the ICRF antennas are proportional to the local plasma density and to the applied RF voltage, and decay exponentially with increasing antenna-plasma distance.

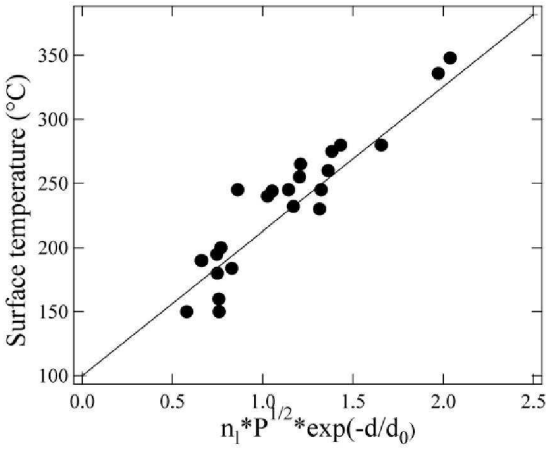


Figure 1: Parametric dependence of surface temperature of Tore Supra Q1 antenna [1].

At present, realistic ICRF antenna codes do not include sheath effects. TOPICA [2] combines accurate 3D modeling of ICRF antennas with a realistic 1D hot plasma model [3]. Its typical output is the scattering matrix and the currents on the conductors. The goal of the present work is to adapt TOPICA such that it can accurately predict detrimental sheath effects such as hot spots on the antenna.

## Sheath Boundary Condition

The general idea is to replace the boundary condition $\mathbf{E}_t = 0$ at the metal conductors by a boundary condition for the sheath-plasma boundary [4]. The sheath region does not need to be modeled explicitly anymore since the boundary condition will contain all sheath effects.

Our interest is in heating and sputtering due to ion acceleration by the rectified RF potential (DC voltage). Therefore the sheath is modeled as a static layer with width $\Delta = \lambda_e \left(\frac{e(V_{sh}+V_{Bohm})}{T_e}\right)^{3/4}$ (Child-Langmuir law). In the limit of inertia-free electrons and immobile ions ($\omega_{pi} < \omega < \omega_{pe}$) the main effect of the electron-poor sheath is to eliminate the large parallel electron currents associated with the RF waves. The RF wave therefore sees the sheath as a vacuum layer and the model treats the sheath as a scalar medium with dielectric constant $\varepsilon_{sh} = 1 + i\nu_{sh}$. The term $\nu_{sh}$ is chosen such that the power absorption in the sheath, given by $P_{sh} = \frac{1}{2}\mathrm{Re}(\sigma_{nn})|E_n^{sh}|^2 A_t \Delta =$

$\frac{\omega \nu_{sh}}{8\pi}|E_n^{sh}|^2 A_t \Delta$, is equal to the power lost by the ions accelerated in the DC sheath potential, given by $P_{sh} = Z n_e c_s T_e h(\xi) \frac{I_1(\xi)}{I_0(\xi)} A_\perp$, with $\xi = ZeV_{sh}/T_e$. For large $V_{sh}$ this goes to $n_e c_s\, ZeV_{sh}\, A_\perp$, with the simple physical interpretation that it is the power dissipated on the antenna surface by ions entering the sheath at velocity $c_s$ and gaining an energy of $ZeV_{sh}$ before reaching the wall.

The thin sheath approximation is used, i.e. the RF wavelength is long compared to the sheath width, $k_t \Delta \ll 1$. The potential in the sheath then increases linearly with distance normal to the surface such that $\nabla_n \phi = \phi_{sh}/\Delta$, where $\phi_{sh}$ is the total potential difference across the sheath.

It is now easy to derive the sheath boundary condition. Continuity of the displacement vector at the sheath-plasma interface gives $D_n^{(pl)} = D_n^{(sh)} = \varepsilon_{sh} E_n^{(sh)} = -\varepsilon_{sh} \nabla_n \phi$. Using the thin sheath approximation, such that $\nabla_n \phi = \phi_{sh}/\Delta$ leads to $\phi_{sh} = -\Delta \frac{D_n^{sh}}{\varepsilon_{sh}}$. Take the tangential gradient to obtain the tangential electric field at the sheath-plasma boundary, $\mathbf{E}_t^{(sh)} = \nabla_t \left( \frac{\Delta}{\varepsilon_{sh}} D_n^{(pl)} \right)$. Finally, continuity of $\mathbf{E}_t$ gives

$$\mathbf{E}_t^{(pl)} = \nabla_t \left( \frac{\Delta}{\varepsilon_{sh}} D_n^{(pl)} \right) \qquad (1)$$

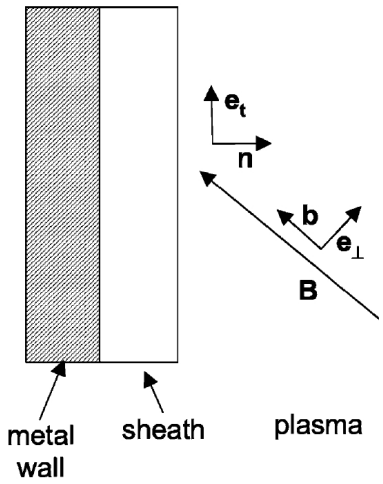

Figure 2: Model geometry.

This 'sheath boundary condition' defines the relationship between the electric field components at the sheath-plasma boundary. Existing antenna codes can be adapted to satisfy the sheath boundary condition instead of the PEC condition, $\mathbf{E}_t = 0$.

**Implementation into TOPICA**

TOPICA uses the PEC boundary condition $\mathbf{E}_t = 0$ and assumes vacuum inside the antenna box. Implementing the sheath boundary condition will require implementing eq. (1), and calculating the fields on the parts of the antenna surface in contact with plasma using a plasma dielectric tensor, i.e. using a plasma Green's function instead of the vacuum Green's function. As an intermediate step the constraint (1) has been implemented but the fields in the antenna box are still calculated in vacuum. Plasma still enters in the sheath parameters $\Delta$, $V_{sh}$ and $P_{sh}$ and enters in $\mathbf{E}_t^{(pl)} = \nabla_t \left( \frac{\Delta}{\varepsilon_{sh}} D_n^{(pl)} \right)$ through $D_n^{pl} = \mathbf{n} \cdot \overleftrightarrow{\varepsilon_{pl}} \cdot \mathbf{E}$. But the wave propagation is calculated for vacuum conditions. We use the thin sheath approximation $k_t \Delta \ll 1$ (and assume $\Delta \ll$ antenna dimensions) to collapse the sheath region in the RF wave field calculations, i.e. the original antenna mesh is used as the computational boundary (= the sheath-plasma boundary).

TOPICA itself is a linear code but by including the sheath boundary condition the calculation becomes non-linear due to the non-linearity in the sheath parameters. An iterative scheme is set up to obtain the solution, as follows. TOPICA is first solved for $\Delta = 0$, which is identical to the

PEC case where $\mathbf{E}_t = 0$. The result of the TOPICA run is the current and field distribution at the sheath-plasma boundary. With these fields a new estimate of $\Delta$, $\nu_{sh}$ and $P_{sh}$ can be obtained.

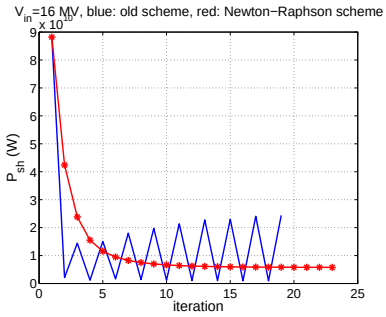


Figure 3: Convergence improvement due to Newton-Raphson scheme.

TOPICA is then run again with these new sheath parameters, and the resulting fields will give a new estimate for $\Delta$ and $P_{sh}$. This sequence is repeated until convergence is reached, e.g. convergence of total dissipated power on the antenna.

At each TOPICA run, the interaction matrix changes due to the new estimates for $\Delta$. A large part of the interaction matrix remains constant however, which is exploited by using 'inversion by partitioning' to speed up the inversion process. A Newton-Raphson scheme is also necessary to obtain satisfactory convergence (note, Fig. 3 obtained for $\overleftrightarrow{\varepsilon}_{pl} = \overleftrightarrow{\varepsilon}_{vac}$).

## First Results

For testing purposes, an idealised situation is considered where plasma would fill the whole antenna box. The sheath boundary condition is implemented at the 4 side walls of the antenna box. At the other conductors the condition $\mathbf{E}_t = 0$ is kept. A simple doubleloop recessed antenna was used, fed in dipole at 48 MHz, short-circuited at the center of the strap. The confinement magnetic field is purely toroidal, parallel to the short edge of the antenna box, $\mathbf{B} = B_0\hat{x}$, with $B_0 = 1$ T.

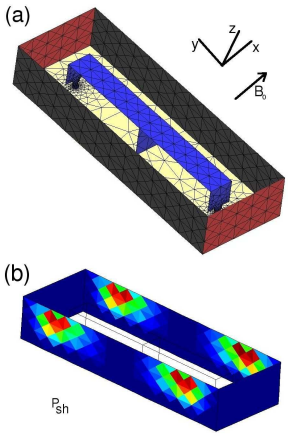


Figure 4: (a) Geometry of test antenna. (b) Distribution of $P_{sh}$.

Fig. 4(b) shows the distribution of the dissipated power on the antenna. This type of plot shows the highest local sheath dissipation, where damage to the antenna might occur. Based on this the design of antennas can be adapted in order to avoid hot spots. This type of plot will also enable direct comparisons with the experimentally measured surface temperature distribution on the antenna (e.g. measured with IR cameras).

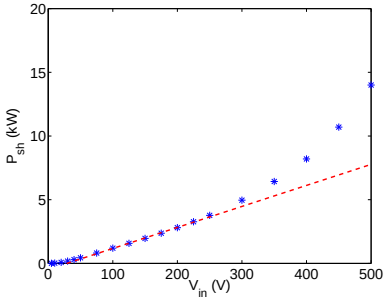


Figure 5: Dependence of $P_{sh}$ on input voltage.

The parametric dependence of the total dissipated power on the antenna with respect to input voltage and density was investigated. The scaling with input voltage $V_{in}$ was done for a plasma with $n = 5\ \ 10^{10}$ cm$^{-3}$ and $T_e = 10$ eV. For very small $V_{in}$ we find $P_{sh} \sim V_{in}^2$. For intermediate $V_{in}$ we find $P_{sh} \sim V_{in}$. This is consistent with experimental observations (see Fig. 1). Note that from the sheath parameter equations it follows that $P_{sh} \sim (D_n^{pl})^4$ for large $D_n^{pl}$. Without the sheath boundary equa-

tion, so with $\mathbf{E}_t = 0$, one would have $D_n^{pl} \sim V_{in}$ and $P_{sh} \sim V_{in}^4$. The action of the sheath boundary equation is to introduce a non-zero tangential field $\mathbf{E}_t$ (rotating the electric field vector away from the magnetic field direction), thereby reducing $E_\parallel$ and reducing $D_n^{pl}$. This shielding of $E_\parallel$ results in $P_{sh} \sim V_{in}$ instead of $P_{sh} \sim V_{in}^4$, consistent with experiments. In the simulation however $P_{sh}$ increases non-linearly again at high $V_{in}$ (still under investigation, possibly a numerical bug).

A comment needs to be made on the size of the input voltages, used in the simulations. As mentioned in the previous section, the fields in the antenna box are calculated in vacuum and the plasma enters only in the sheath equations through $D_n^{pl} = \mathbf{n} \cdot \overleftrightarrow{\varepsilon}_{pl} \cdot \mathbf{E}$. The vacuum field $E_\parallel$ is of the same order as $E_\perp$, and therefore $D_n^{pl}$ will be overestimated since $E_\parallel$ is too large in the term $\varepsilon_\parallel E_\parallel$. As a result, the sheath dissipation will be very large already at low input voltages of a few hundred volts. In the next implementation step, the vacuum Green's function now used in the antenna box will be replaced by the plasma Green's function, whereby $E_\parallel$ will decrease by a factor on the order of $\sqrt{M/m} \sim 40$. We then expect to see similar size sheath dissipation for input voltages a factor of $\sqrt{M/m}$ higher, i.e. input voltages on the order of 20 kV.

The scaling of the sheath dissipated power with the local density was done for $V_{in} = 50$ V and $T_e = 10$ eV. As expected, higher densities lead to higher sheath dissipated power since the influx of plasma-ions into the sheath and accelerated to the plates is higher. Except at very low densities, the simulation shows a linear increase of $P_{sh}$ with density, consistent with experimental observations (see Fig. 1).

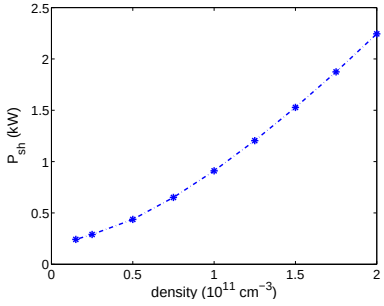

Figure 6: Dependence of $P_{sh}$ on density.

## Conclusions

Recent experiments on hot spots in ICRF antennas stress the importance of including sheath effects into antenna codes. The present work implements a sheath boundary condition into the antenna code TOPICA. The first step involves the implementation of the sheath boundary condition but with the fields in the antenna box still calculated in vacuum. The preliminary results are encouraging, and are able to reprodruce the experimentally observed parametric dependences.

## References

[1] L. Colas *et al*, Nuclear Fusion **46**, S500-S513 (2006)

[2] V. Lancellotti *et al*, Nuclear Fusion **46**, S476-S499 (2006)

[3] M. Brambilla, Nuclear Fusion **35**, 1265-1280 (1995)

[4] D. A. D'Ippolito and J. R. Myra, Physics of Plasmas **13**, 102508 (2006)